

Supplementary Material for Emberson et al. 2021 - Topographic characteristics of rainfall-induced landslides

Supplementary Figures

Next set of figures: pair-plots for each of the analysed parameters, to show the presence or absence of co-linearity.

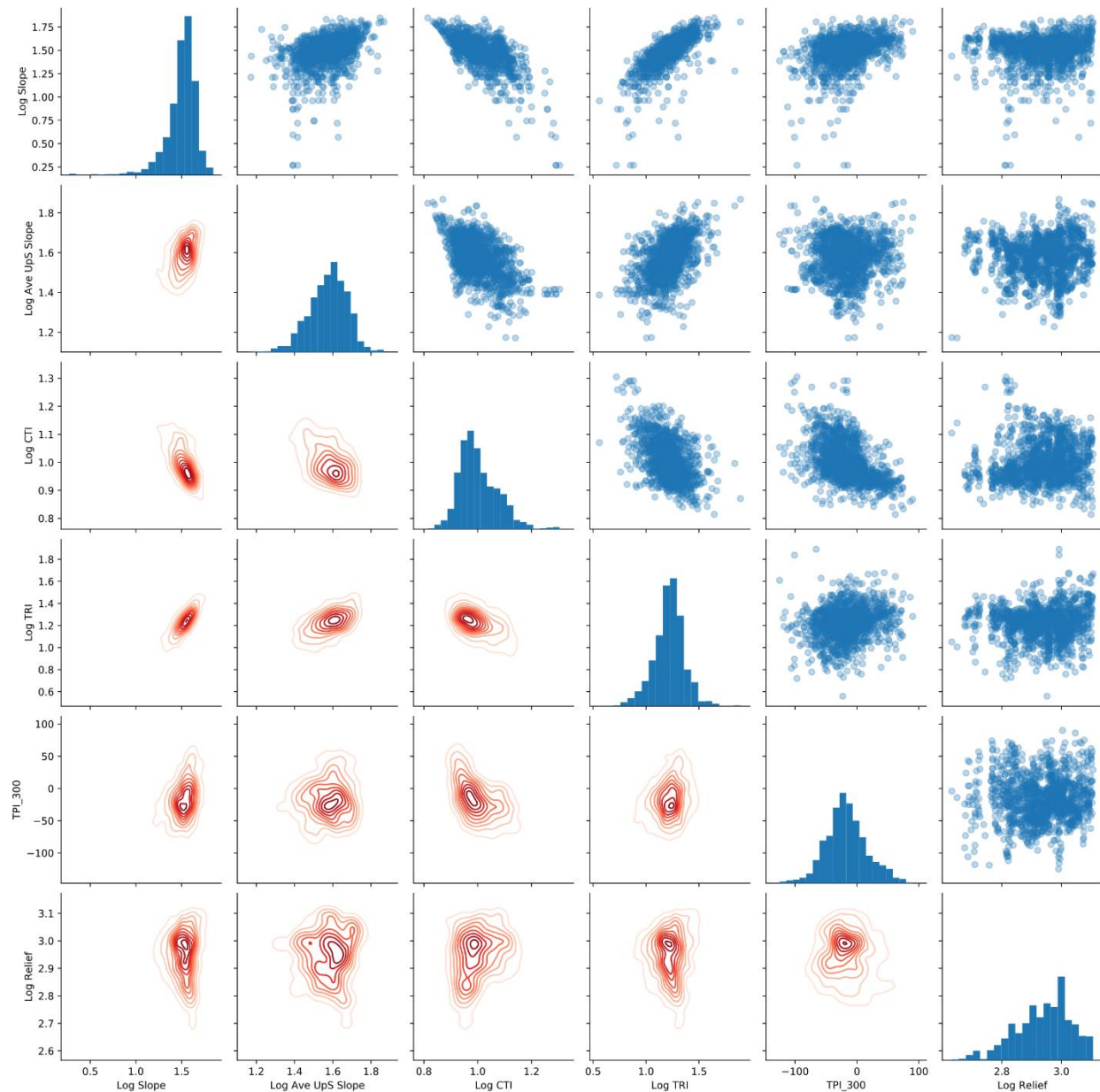


Figure S1: Pair-plots and heatmaps for landslide data for each of the parameters considered. Central diagonal shows the histogram for each parameter, while the upper right quadrant shows the pair-plots

for the pixels in each dataset. Bottom left quadrant shows the same data, but as a contour-plot, with the denser contours indicating higher numbers of points in that part of the figure.

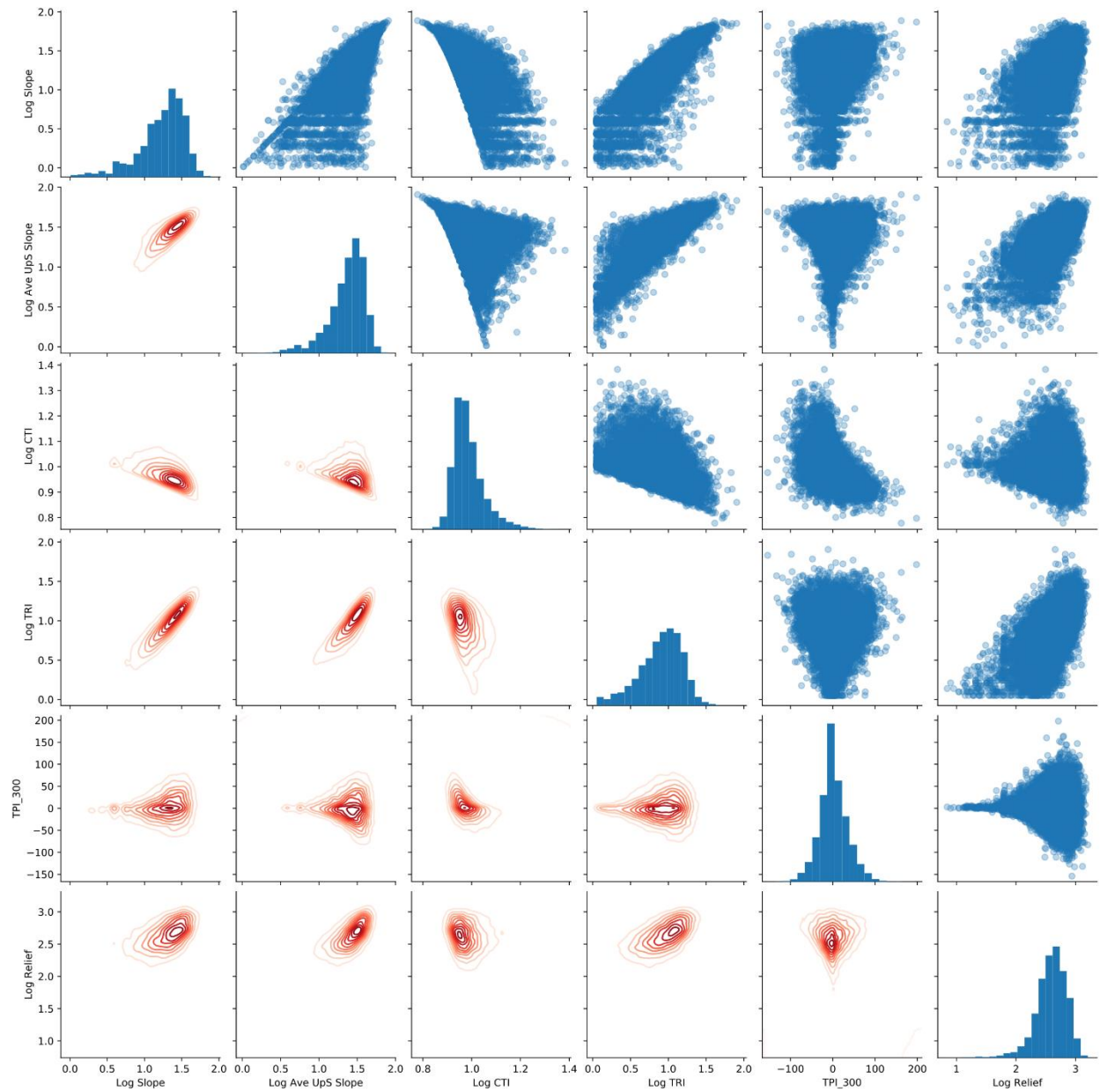


Figure S2: This figure shows the relationships for the topographic variables for the entire landscape area for all study areas. This shows a random subset of 2000 pixels from the mapped areas for each of the inventories.

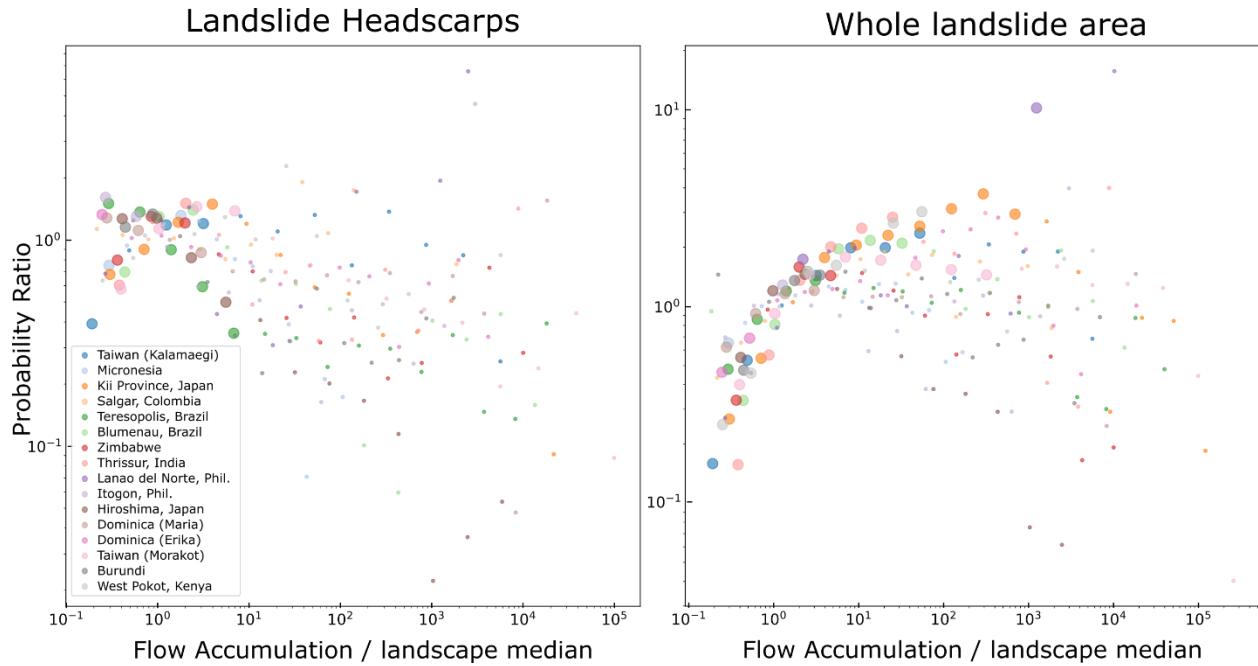


Figure S3: Probability ratios of flow accumulation for landslide headscarps and whole landslide areas, normalized by the median of slope value for the area covered by the inventory.

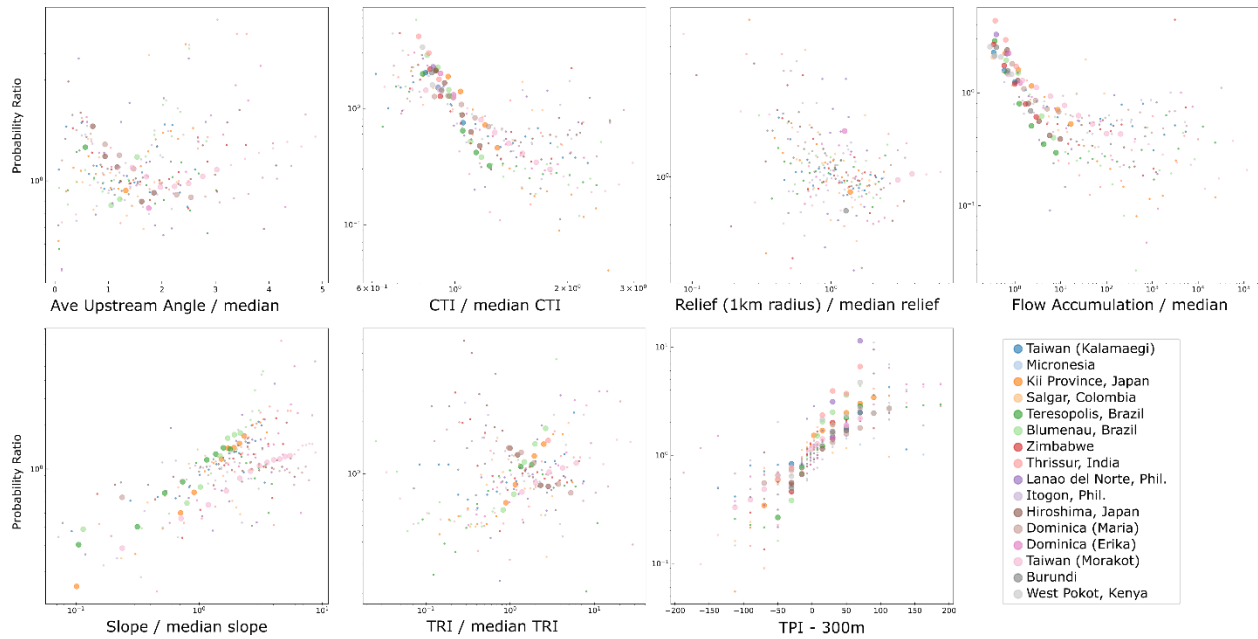
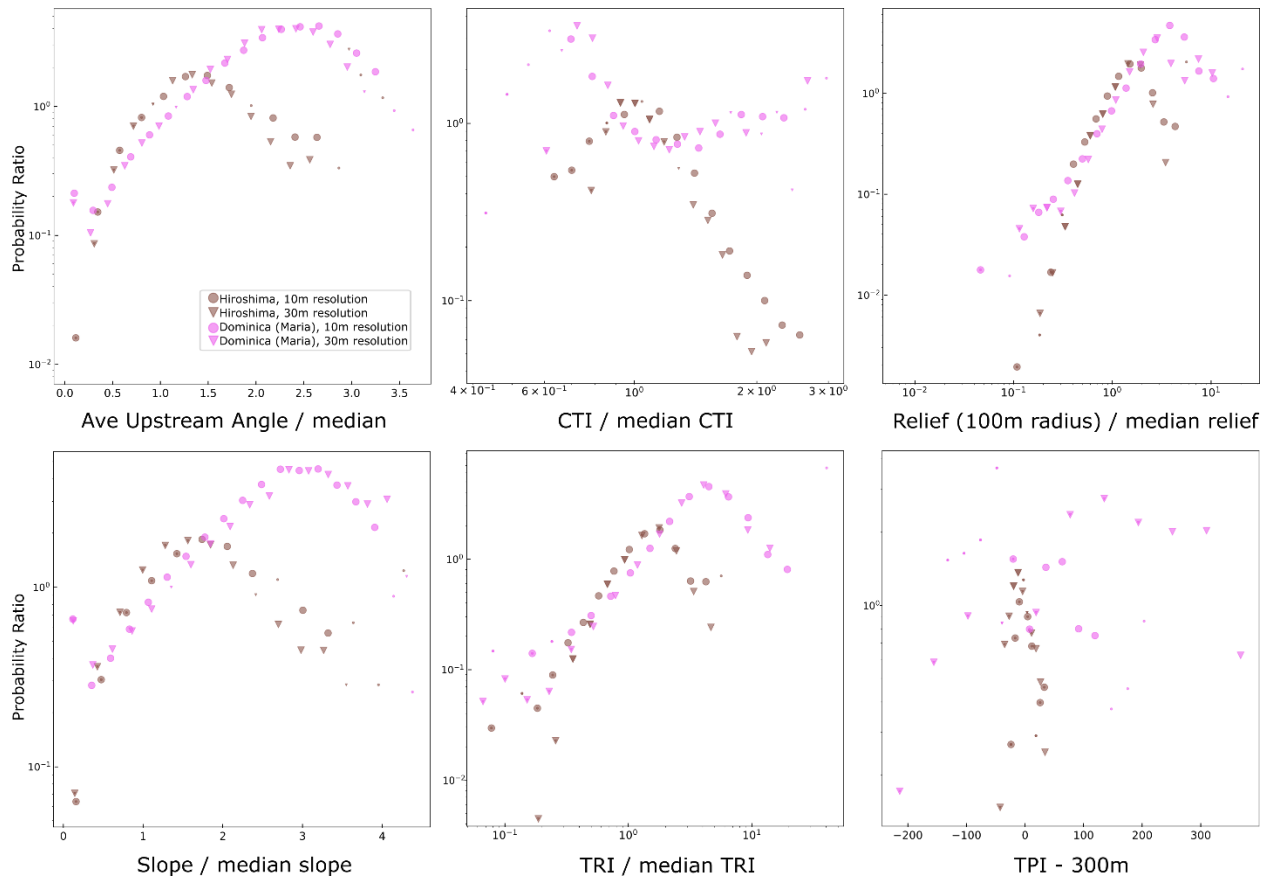


Figure S4: Ratio of headscarp areas to whole landslide areas, for each of the measured parameters. Higher y-axis values indicate that those values are more common in headscarps, while lower y-axis values indicate those values are more common in the whole landslide body. Note that for each of the parameters with x-axis labels including 'divided by median' this means that the values are normalised by the median value for that parameter in the entire mapped area. For TPI this is not carried out.



Supplementary Figure 5: Difference in probability ratios if DEM is resampled to 10m resolution for the entire landslide area. Results are shown for the two inventories where small landslides make up an appreciable proportion of the overall area occupied by landslides (Hiroshima, and landslides from Hurricane Maria in Dominica).

Supplementary Figures 6-11: Satellite images of new landslide inventories

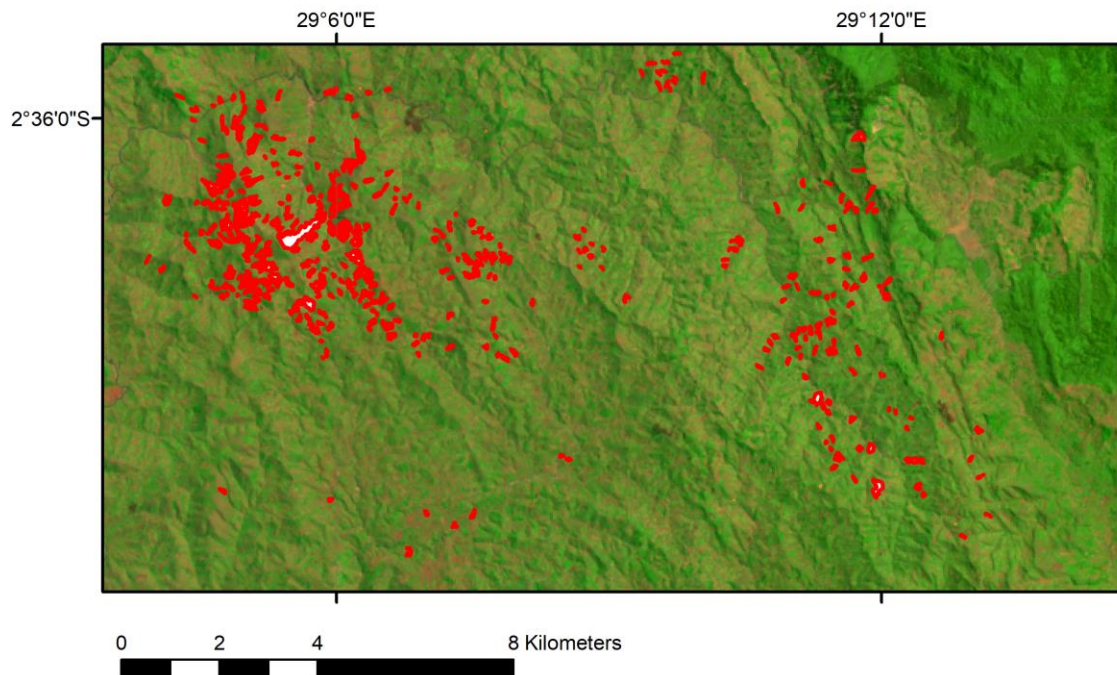


Figure S6: Distribution of landslides in the Burundi landslide inventory, presented here for the first time. Red outlines show landslides. Underlying imagery: Sentinel 2

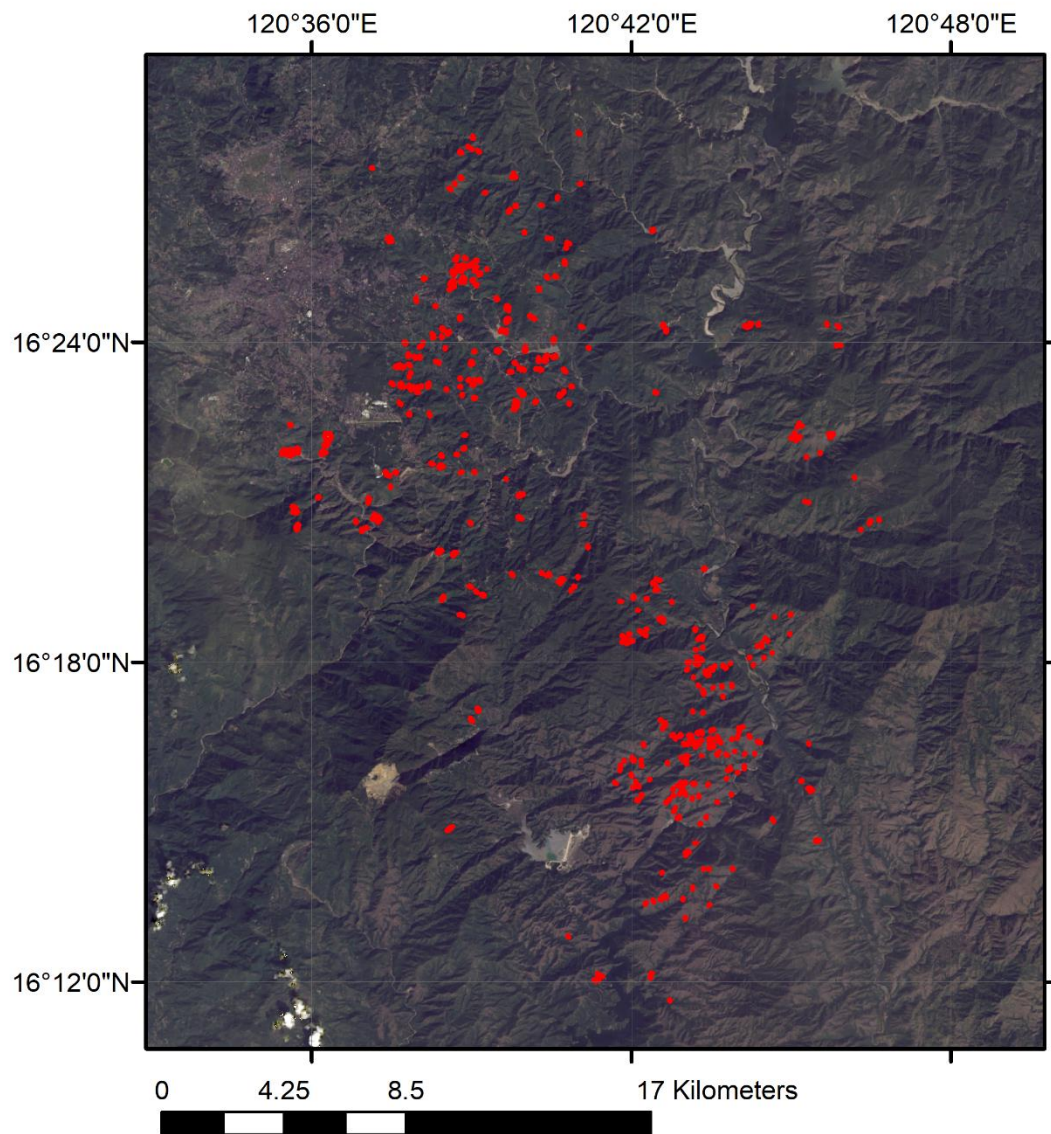


Figure S7: Distribution of landslides in the inventory from Itogon, Philippines, presented here for the first time. Red outlines show landslides. Underlying imagery: LandSat 8 OLR true color.

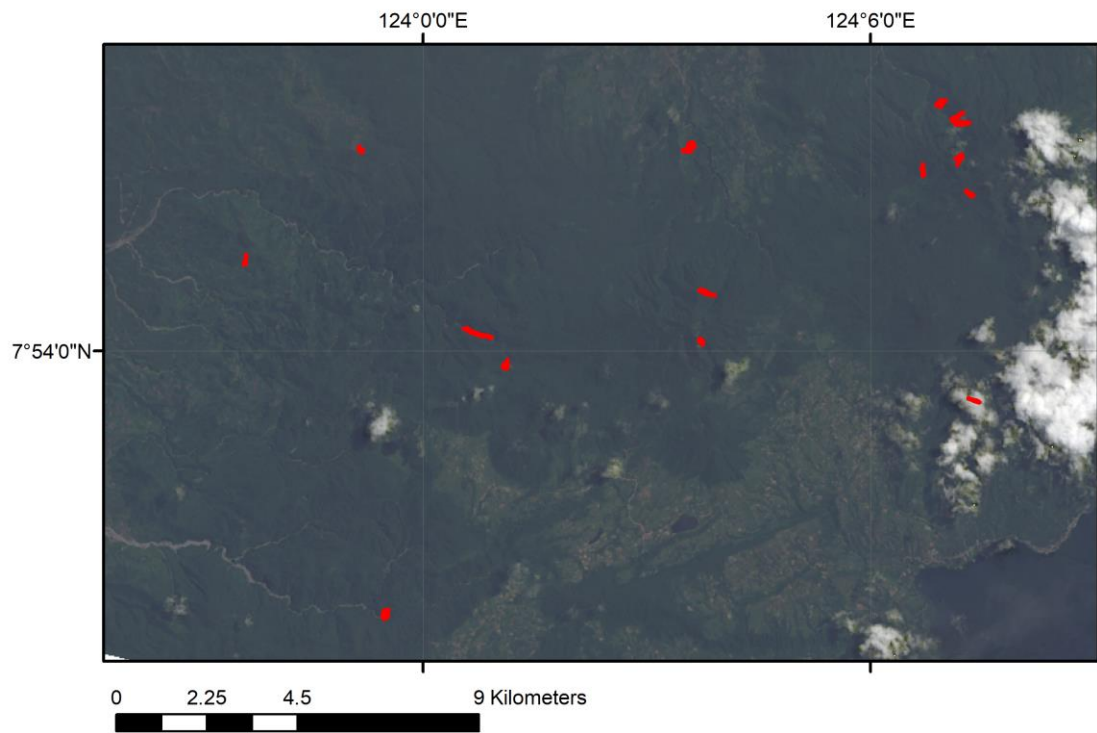


Figure S8: Distribution of landslides in the inventory from Lanao del Norte, Philippines, presented here for the first time. Red outlines show landslides. Underlying imagery: LandSat 8 OLR true color.

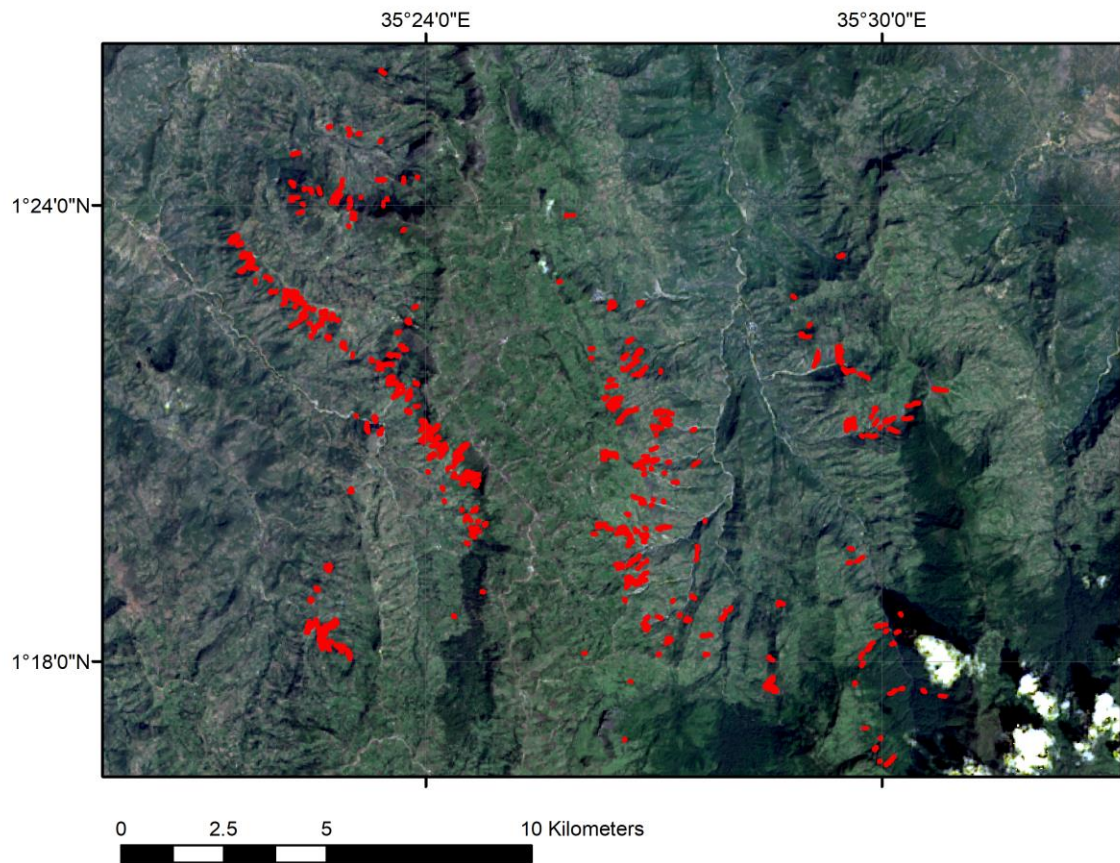


Figure S9: Distribution of landslides in the inventory from West Pokot, Kenya, presented here for the first time. Red outlines show landslides. Underlying imagery: LandSat 8 OLR true color.

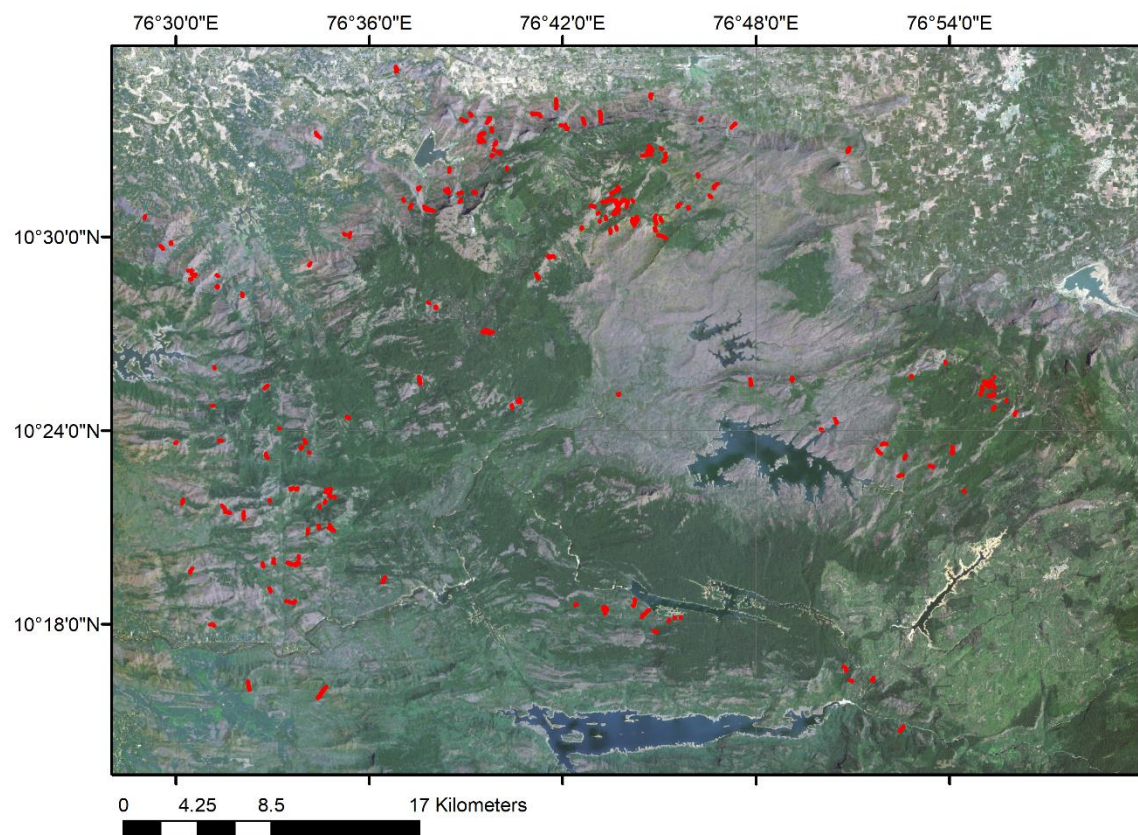


Figure S10: Distribution of landslides in the inventory from Thrissur, India, presented here for the first time. Red outlines show landslides. Underlying imagery: LandSat 8 OLR true color.

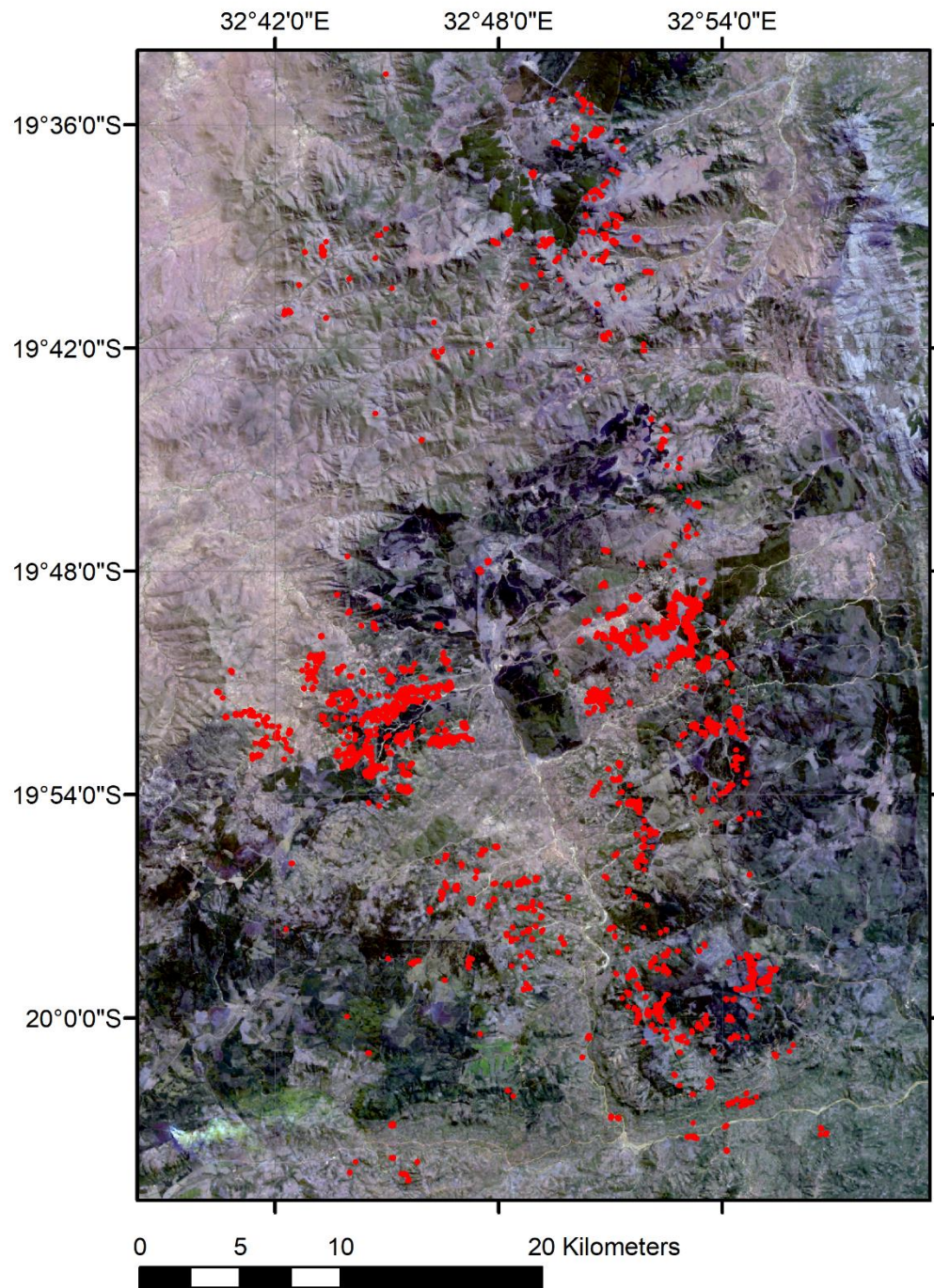


Figure S11: Distribution of landslides in the inventory triggered by Cyclone Idai in Zimbabwe, presented here for the first time. Red outlines show landslides. Underlying imagery: LandSat 8 OLR true color.

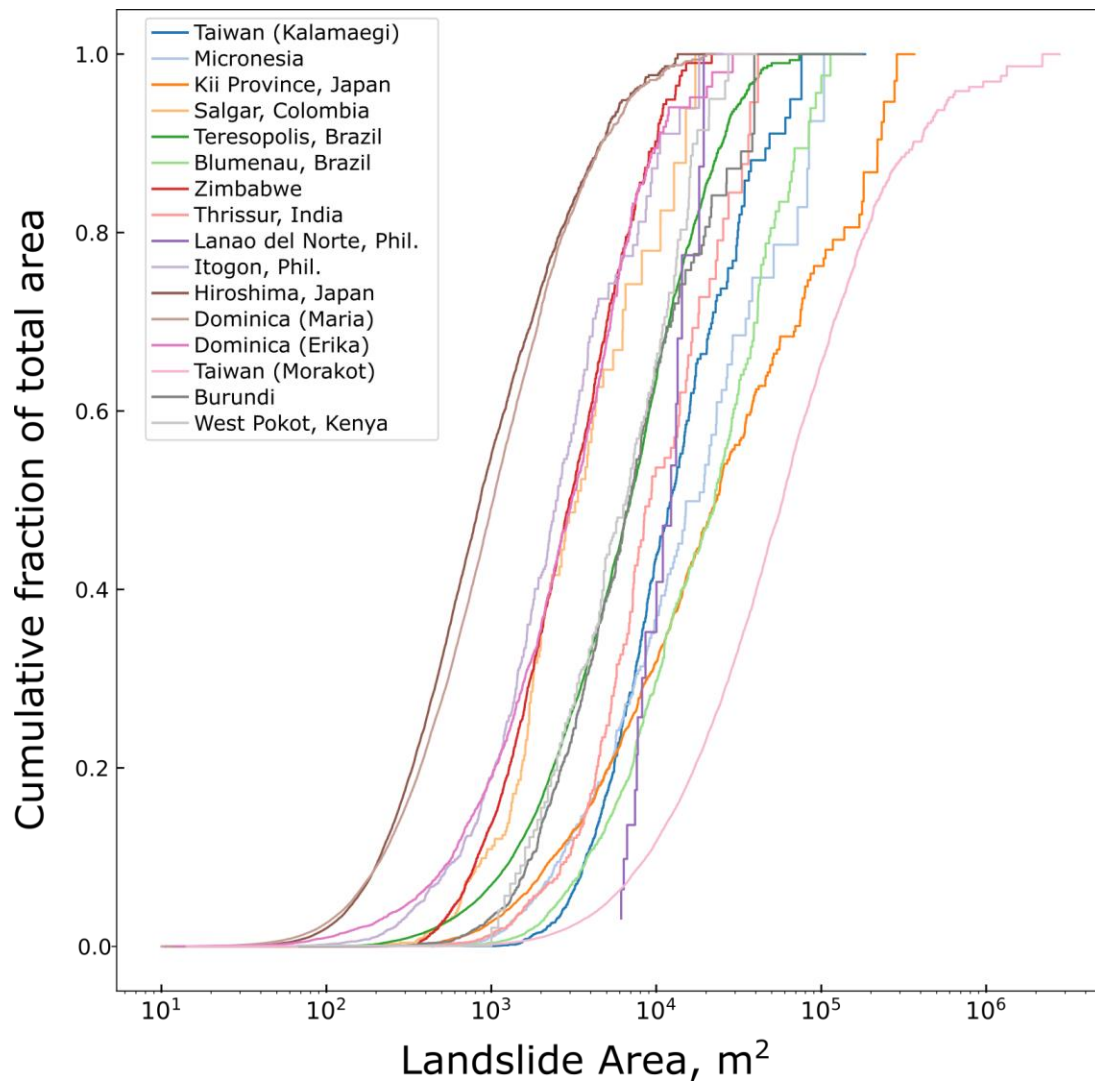


Figure S12: Showing the proportion of the total landslide area for each inventory that is contributed by landslides of a given size. In two cases, Dominica (Maria) and Hiroshima, Japan, landslides smaller than 450 m^2 make up a large proportion of the overall landslide area.